Article ID: 1000-7032(2022)10-1628-08

Utilizing NIR AIE Luminogen Based Magnetic Nanoparticle for Light-enhanced Bacterial Killing

XIE Hong-qin[1], XIE Yang-zi[2], WANG Yue-ting[2], JIAO Zhe[2*], GUO Zong-ning[3], HUANG Xue-lin[3*], CHEN Ming[4], LUO Xiao-zheng[2]

(1. *Guangdong Dongguan Ecological and Environmental Monitoring Station, Dongguan* 523106, *China*;
2. *Dongguan University of Technology, Dongguan* 523808, *China*;
3. *Huangpu Customs District Technology Center, Dongguan* 523000, *China*;
4. *College of Chemistry and Materials Science, Jinan University, Guangzhou* 510632, *China*)

* *Corresponding Authors, E-mail: jiaoz@dgut. edu. cn*; 34056583@*qq. com*

Abstract: NIR photosensitizers(PSs) could significantly improve the efficacy of photodynamic therapy due to the long-wavelength favorability for deeper tissue penetration and lower biological damage. In this paper, a deep-red emissive AIEgens 5,6-bis(4′-(diphenylamino)-[1,1′-biphenyl]-4-yl) pyrazine-2,3-dicarbonitrile(DCDPP-2TPA) was synthesized for light-enhanced bacterial killing. Due to the advantage of AIEgens which are ultra-emissive in the aggregate states or solid states, DCDPP-2TPA was incorporated into magnetic nanoparticle to increase aggregation enhanced reactive oxygen species(ROS) generation property as well as magnetic separation convenience. The magnetic particles were studied by scanning electron microscope(SEM), transmission electron microscope(TEM), X-ray diffraction(XRD), and fluorescence spectrophotometer, *etc*. The capacity of bacterial killing was exhibited on *E. coli* and *S. aureus* under light irradiation. Due to the aggregation enhanced ROS generation, the viability of *E. coli* and *S. aureus* treated with DCDPP-2TPA based magnetic nanoparticle with room light illumination for 30 min are 7.5% and 9.0%, which was superior to DCDPP-2TPA(10% and 14% respectively). The significant superiority of magnetic nanoparticles is that it can be withdrawn easily and continuously used for bacteria killing by applying light to induce ROS generation.

Key words: AIE luminogen; magnetic nanoparticle; bacterial killing

CLC number: O482.31 **Document code**: A **DOI**: 10.37188/CJL.20220015

基于近红外聚集诱导发光分子的磁性纳米材料用于光增强杀菌

谢宏琴[1], 谢样梓[2], 王玥婷[2], 焦 哲[2*], 郭宗宁[3], 黄雪琳[3*], 陈 明[4], 罗孝铮[2]

(1. 广东省东莞生态环境监测站, 广东 东莞 523106; 2. 东莞理工学院 生态环境与建筑工程学院, 广东 东莞 523008;
3. 黄埔海关技术中心, 广东 东莞 523000; 4. 暨南大学 化学与材料学院, 广东 广州 510632)

摘要: 近红外光敏剂由于荧光成像具有光损伤小、穿透力强和空间分辨率高等优点,能显著提高光动力治疗效果。我们合成了近红外聚集诱导探针5,6-2(4′-(二苯氨酚)-[1,1′-联苯]-4-yl) 吡嗪-2,3-二甲腈(DCDPP-2TPA)

收稿日期: 2022-05-21; **修订日期**: 2022-06-06
基金项目: 广东省科技厅海外名师项目(2021441900000); 东莞市社会发展科技项目面上项目(20211800901582); 东莞市科技特派员项目(20201800500172); 东莞市社会发展科技项目重点项目(2019507101162); 广东省科技计划(2018B020208005)资助项目
Supported by Guangdong Oversea Prominent Teachers Project (2021441900000); Dongguan Social Development Science and Technology Project General Project (20211800901582); Dongguan Science and Technology Commissioner Project (20201800500172); Key Project of Dongguan Social Development Science and Technology Project (2019507101162); Guangdong Provincial Science and Technology Project(2018B020208005)

用于光增强杀菌。利用聚集态/固态下荧光增强的优势,DCDPP-2TPA与磁性Fe_3O_4纳米材料复合,产生更高活性氧(ROS)用于杀菌。利用SEM、TEM、XRD和荧光光谱研究了该复合材料的结构和性质,并用于大肠杆菌和金黄色葡萄球菌杀菌实验。结果表明,在光照下两种细菌的存活率为7.5%与9.0%,优于DCDPP-2TPA(10%与14%)。同时该复合材料可以方便地实现磁性分离,在光照下产生ROS后循环杀菌。

关　键　词: 聚集诱导发光; 杀菌材料; 磁性纳米材料

1　Introduction

Outbreaks of waterborne pathogens (such as Escherichia coli (*E. coli*), Staphylococcus spp. and Salmonella spp.) regularly occur especially during epidemic situation, war fare or natural disasters. Due to the very low infection dose (around 100 organisms) and given the biological diversity of harmful pathogens, it is a continual challenge to prevent infectious disease outbreaks. Antibiotics are the most widely used materials for pathogen prevention and infection treatment, but are becoming less efficient due to the emergence of antibiotic-resistant bacterial strains[1]. Recently, nanomaterials such as TiO_2, Ag_2O, have been an alternative, but its second pollution has been found[2]. Therefore, it is crucial to develop reusable, safe and convenient material, especially applied in the emergent occasion.

Photodynamic therapy (PDT) is a potential alternative to antibiotics to kill bacteria[3-5]. In general, PDT employs photosensitizers to absorb light and generate single excited state (S1), then the S1 state can further transfer the energy to triplet excited state (T1), which would sensitize the ambient triplet oxygen, resulting in formation of the destructive singlet oxygen or other reactive oxygen species (ROS)[6-7]. PDT can target both external and internal structures of bacteria, and not really requires the photosensitizers to enter bacteria, thus, the sterilization mechanism of PDT is different from traditional antibiotics[8]. Therefore, bacteria can hardly develop resistance to PDT[9]. The conventional photosensitizers suffered from the notorious aggregation-caused quenching (ACQ) effect after they accumulated, which will lead to the reduction in their fluorescence intensities in the solid state, thus seriously eroding the performance. The concept of AIE (aggregation-induced emission) was coined by Tang's group in 2001[10-11]. The aggregation-induced emission fluorogens(AIEgens) are non-emissive in dilute solution but emit intensely upon aggregate formation, which are very suitable for solid-state application. The unique properties of AIEgens make them excellent candidates for fluorescent nanoparticle development[12].

Development of AIEgens to exhibit ROS generation ability and applications in PDT has been reported recently[13-16]. NIR AIEgens could be excited by simultaneously absorbing long-wavelength photons. This unique character is advantageous for PDT, due to its deeper penetration power, lower cell radiation and less background fluorescence leading to better signal to noise ratio. However, there are only a few reports of such materials for three-photon PDT applications, due to low optical stability and complex synthesis. As reported in our previous literature, a deep-red emissive AIEgen 5,6-bis(4′-(diphenylamino)-[1, 1′-biphenyl] -4-yl) pyrazine-2, 3dicarbonitrile (DCDPP-2TPA) was synthesized, which exhibited bright three-photon fluorescence signals with deep-red emission molecules and high photostability due to absence of nonaromatic double bonds in DCDPP-2TPA molecules[17]. It was applied for through-skull fluorescence microscopic imaging of mouse cerebral vasculature without craniotomy and skull-thinning. However, its potentiality for bacterial killing has never been explored.

Through encapsulating AIEgens within a certain matrix to form nanoparticles (NPs), the intramolecular motions of AIE molecules can be suppressed, and the fluorescence quantum yield, especially aggregation enhanced property is greatly improved. The condensed particles can also largely reduce the photo-oxidation of dye molecules by keeping the oxygen out. Among different NPs, magnetic NPs(MNPs)

show great advantage for quick separation once completed. Therefore, it is expected that by incorporating ROS generation AIEgens with magnetic NPs, novel multifunctional bacteria-killing materials will be developed for portable on-site application.

Herein, based on the NIR AIEgens (DCDPP-2TPA) that has been reported by our group, we further developed multifunctional MNPs as PDT agents for bacterial killing. The structure of the MNPs was studied. The ROS generation property of DCDPP-2TPA was examined by SOSG. Finally, it was applied for Gram-negative bacteria *E. coli* and Gram-positive bacteria *S. aureus* killing in water.

2 Experiment

2.1 Chemicals and Regents

Sodium hydroxide, ferrous chloride, ferric chloride, 2,3-diaminomaleonitrile and dimethyl sulfoxide (DMSO) were purchased from Tianjin Damao Chemical Reagent Company. Ethyl acetate, methanol, tetrahydrofuran, sodium dodecyl benzene sulfonate(SDBS) and sodium chloride were obtained from Tianjin Fuchen Chemical Reagent Company. Agar powder, tryptone and beef extract were bought from Beijing Baolai Tech Co., Limited. Singlet oxygen sensor green (SOSG) was bought from Shanghai Maokang Biotech Co., Limited. 1,2-bis(4′-(diphenylamino)-[1,1′-biphenyl]-4-yl) ethane-1,2-dione (**1**) was obtained in our previous work[17].

2.2 Synthesis of 5,6-Bis(4′-(diphenylamino)-[1,1′-biphenyl]-4-yl)pyrazine-2,3-dicarbonitrile(DCDPP-2TPA, 2)

The synthetic route DCDPP-2TPA(**2**) was provided in the supporting information(Fig. S1). 1,2-bis(4′-(diphenylamino)-[1,1′-biphenyl]-4-yl)ethane-1,2-dione(**1**, 500 mg, 0.72 mmol), 2,3-diaminomaleonitrile(**2**, 85 mg, 0.79 mmol) and 30 mL of acetic acid were added into a 100 mL round-bottom flask. The mixture was stirred at reflux for 12 h. Afterwards, the mixture was cooled down to the room temperature and poured into the ice water. Then, the dichloromethane was added and the red organic phase was collected followed by washing with water three times. The organic phase was concentrated by reduce pressure and the product was purified by a silica gel column using dichloromethane/petroleum ether(*v*/*v* = 1∶2) as eluent. A red powder of DCDPP-TPA was obtained in a yield of 72.3%. ^{1}H NMR(300 MHz, CD_2Cl_2): 7.73−7.64(m, 8H), 7.58−7.55(d, 4H), 7.35−7.30(t, 8H), 7.16−7.08(m, 16H). ^{13}C NMR (75 MHz, $CDCl_3$): 154.8, 148.2, 147.4, 143.4, 133.5, 132.6, 130.4, 129.4, 127.8, 126.8, 124.8, 123.4, 123.3, 113.3. HRMS(MALDI-TOF): *m*/*z* 768.299 9 [M^+, calcd for 768.300 1](Fig. S2, S3, S4).

2.3 Preparation of DCDPP-2TPA Based MNPs

Sodium hydroxide was first prepared in aqueous solution (0.605 mol/L). Then ferrous chloride and ferric chloride were mixed and dissolved (concentrations were 0.05 mol/L and 0.10 mol/L respectively) and equipped in the microwave-ultrasonic system. After reaction for 1 h at 40 ℃, the sodium hydroxide solution was added drop by drop in N_2 atmosphere. Finally, the resultant product Fe_3O_4 MNPs was washed by water for three times and dried overnight for use. For preparation of DCDPP-2TPA based MNPs, SDBS was prepared in aqueous solution (1.2 mmol/L), then 1 mg of DCDPP-2TPA was added and sonicated for 5 min. After that, 1 mL of DMSO was added and sonicated for 10 min. Finally, Fe_3O_4 MNPs(0.018 g) was added and stirred for 2 h. The resultant product DCDPP-2TPA based MNPs was washed and dried in vacuum oven for use.

2.4 Application of DCDPP−2TPA Based MNPs for Bacteria Killing

The prepared medium was poured evenly into six Petri dishes for cooling and solidification. The bacterial (the absorption ODs at 600 nm was 0.5) culture medium was diluted 1 000 times with PBS buffer. 1 mL of each were added to six disposable centrifuge tubes, and following adding of Fe_3O_4 MNP, DCDPP-2TPA and DCDPP-2TPA based MNPs respectively (The mass was all 1.0 mg). Six centrifuge tubes were incubated in the incubator at 37 ℃ for 30 min, and then the light group was exposed to natural light for 30 min. Finally, six centrifuge tubes were centrifuged, 100 μL supernatant from each centrifuge tube was added to the prepared solid medium, and cultured at 37 ℃ for 24 h. All solutions and

materials are autoclaved before use.

The reuse of DCDPP-2TPA based MNPs bacteria killing was studied by magnetic recycling. First, 10 mg of DCDPP-2TPA based MNPs is dispersed in 2 mL of aqueous solution to form a suspension, and then the solution is placed on the magnet for 1 min. After separation of the solution, the DCDPP-2TPA based MNPs was used for next cycle.

3 Results and Discussion

3.1 Characterization of Magnetic Particles

The appearance of the nanoparticles was shown in Fig. S5. It was black particles under nature light and red emissive under UV light, which showed that DCDPP-2TPA had been combined with Fe_3O_4 MNP. The photoluminance spectra (PL) of DCDPP-2TPA, MNPs and DCDPP-2TPA based MNPs were provided in Fig. 1(a). The fluorescence emission at 650 nm was both observed in DCDPP-2TPA, and DCDPP-2TPA based MNPs. Besides, the magnetic curve(Fig. 1(b)) showed the nanoparticles exhibited superparamagnetic property as Fe_3O_4. The micro-morphology of the nanoparticles was studied by transmission electron microscope(TEM) (Fig. 1(c)) and scanning electronic microscopy(SEM)(Fig. 1(d)), the particle was sphere and well-distributed with diameter at about 30–40 nm.

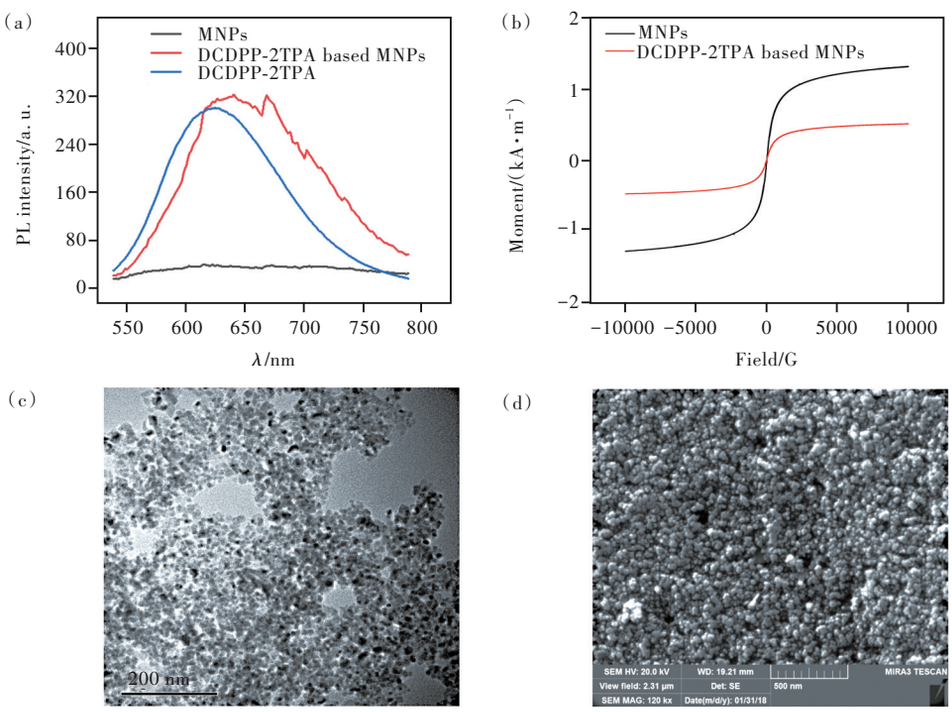

Fig. 1 (a) PL spectra of DCDPP-2TPA, MNPs and DCDPP-2TPA based MNPs. (b) Magnetizing curve of MNPs and DCDPP-2TPA based MNPs. (c) TEM image of DCDPP-2TPA based MNPs. (d) SEM image of DCDPP-2TPA based MNPs.

X-ray diffraction spectrum and IR spectrum were also obtained(Fig. S6). The diffraction peaks at 30.22°, 35.66°, 43.25°, 53.65° and 62.88° in X-ray diffraction spectrum proved the existence of Fe_3O_4. In the IR spectrum of DCDPP-2TPA based MNPs, 574 cm^{-1} and 1 614 cm^{-1} are the Fe—O characteristic stretching vibration peaks of Fe_3O_4 and MNP, but the peaks of DCDPP-2TPA were not observed clearly. It might be because of low mass ratio of DCDPP-2TPA in Fe_3O_4 MNP.

The surface potential of MNPs and DCDPP-2TPA based MNPs were studied(Fig. S6). The results showed that the surface potential increased with the binding of DCDPP-2TPA with MNPs. Besides, the hydrodynamic diameters of MNPs and DCDPP-2TPA based MNPs were measured (Fig. S7). Compared with MNPs, the hydrodynamic particle size of DCDPP-2TPA based MNPs increased, which was caused by the combination of DCDPP-2TPA and MNPs. The coverage amount of DCDPP-2TPA on magnetic nanoparticles was also studied by the comparative absorption ODs at 510 nm(Fig. S9).

It was measured with the reference DCDPP-2TPA solution (1.16×10^{-2} mmol/L) before the insertion of the magnetic particles for reaction and the remaining DCDPP-2TPA solution obtained after the reaction with the particles. The ODs difference indicates that 0.037∶1(mass ratio) of DCDPP-2TPA is immobilized onto the surface of magnetic particles.

3.2 Evaluation of Aggregation Enhanced ROS Generation by SOSG

The mechanism for killing bacteria was based by the singlet-oxygen produced by the DCDPP-2TPA. To investigate the ability to generate $^1O_2$, the $^1O_2$ quantum yield was determined using a chemical trapping method by monitoring the absorption of 9, 10-anthracenediyl-bis(methylene) dimalonic acid at 378 nm, and the $^1O_2$ quantum yield was 12%. SOSG was applied for detection of singlet-oxygen in this system. As seen in Fig. 2, the PL spectra of SOSG was obtained in the presence of DCDPP-2TPA and DCDPP-2TPA based MNPs. In the mixture of SOSG and DCDPP-2TPA, the PL intensity at 530 nm both became stronger with the irradiation time. When the time reached 60 min, the emission became stable. While in the mixture of SOSG and DCDPP-2TPA based MNPs, the PL intensity at 530 nm increased along with prolonged time at 60 min. Due to the aggregation enhanced ROS generation, the PL intensity of SOSG was higher in the presence of MNPs than DCDPP-2TPA alone. The reason might be that the condensed packing of AIE molecules in the nanoaggregates blocks the intramolecular motions, promotes the radiative decay and enhances the emission, therefore AIE MNPs are with intense fluorescence and the emission can be retained after continuous irradiation.

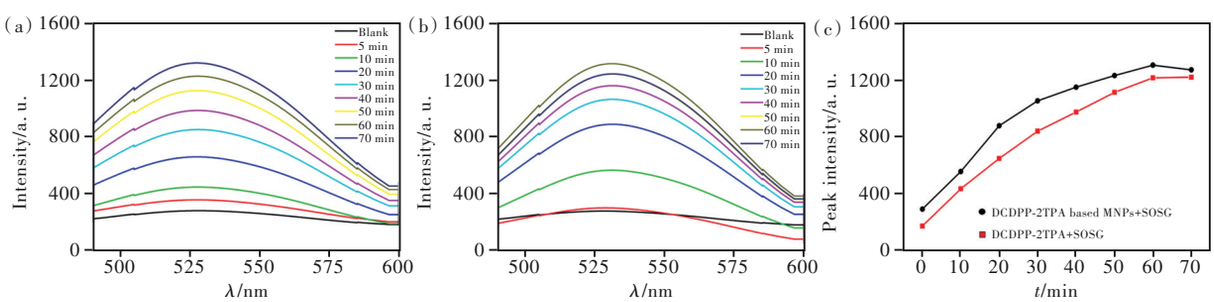

Fig. 2 (a) The PL spectra of SOSG in the presence of DCDPP-2TPA. (b) The PL spectra of SOSG in the presence of DCDPP-2TPA based MNPs. (c) PL intensity change of SOSG in the presence/absence of DCDPP-2TPA.

3.3 Study of the Bacteria Killing by DCDPP-2TPA and DCDPP-2TPA Based MNPs

Gram-negative bacteria *E. coli* and Gram-positive bacteria *S. aureus* were tested to study the killing capacity of DCDPP-2TPA and DCDPP-2TPA based MNPs. The images of plates for the quantification of the killing effect on *E. coli* and *S. aureus* were obtained to gain a direct impression of the killing effect (Fig. 3-4). Without treatment, the bacteria grow healthily on the plate. When treated with DCDPP-2TPA in the dark, the amount of *E. coli* decreased to some extent, but there are still some alive bacteria on the plate(Fig. 3(b)), suggesting the inefficient killing of DCDPP-2TPA without light irradiation. In the presence of both DCDPP-2TPA and light irradiation, *E. coli* was killed effectively and almost no colony forms on the plate, which showed the high bacterial killing efficiency under light irradiation(Fig. 3(e)). A similar effect is observed on

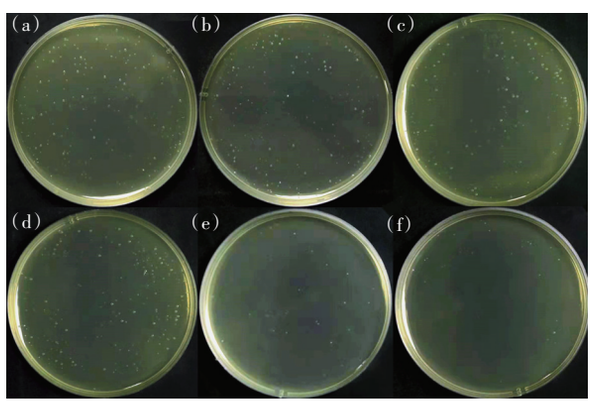

Fig. 3 Plates of *E.coli* under different conditions. (a) Without treatment. (b) Treatment with DCDPP-2TPA in dark. (c) Treatment with DCDPP-2TPA based MNPs in dark. (d) Treatment with MNPs. (e) Treatment with DCDPP-2TPA in light. (f) Treatment with DCDPP-2TPA based MNPs in light.

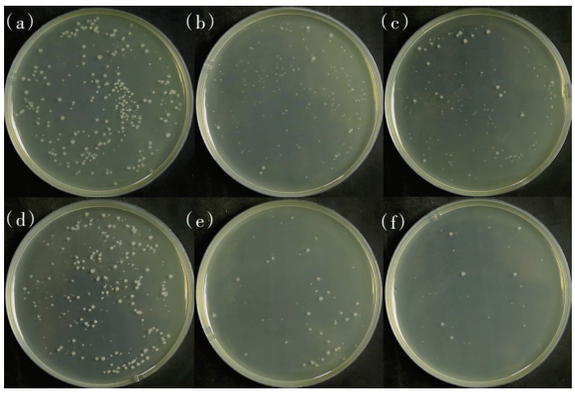

Fig. 4　Plates of *S. aureus* under different conditions. (a) Without treatment. (b) Treatment with DCDPP-2TPA in dark. (c) Treatment with DCDPP-2TPA based MNPs in dark. (d) Treatment with MNPs. (e) Treatment with DCDPP-2TPA in light. (f) Treatment with DCDPP-2TPA based MNPs in light.

the *S. aureus* (Fig. 4). It proved that DCDPP-2TPA could kill both Gram-positive and -negative bacteria efficiently with light irradiation.

The bacterial killing capacity of DCDPP-2TPA based MNPs was studied. Firstly, the effect of Fe_3O_4 MNPs on bacteria viability was investigated in the absence of DCDPP-2TPA. As seen in Fig. 3 and Fig. 4, the *E. coli* and *S. aureus* both remain healthy in the presence of Fe_3O_4 MNPs, showing that the magnetic particle had little effect for killing bacteria. Treatment with DCDPP-2TPA based MNPs in the dark decreases the amount of *E. coli*/*S. aureus* to some extent, but there are still some alive bacteria that can grow to form colonies on the plate, suggesting the inefficient killing in the dark. In the presence of both DCDPP-2TPA based MNPs and light irradiation, both *E. coli* and *S. aureus* are killed effectively and their viability, which is a good sign of high bacterial killing efficiency under light irradiation.

The killing efficiency was further assessed by the plate-count method (Fig. 5). The viability of bacteria remained unchanged in the presence of Fe_3O_4 MNPs, When treated with DCDPP-2TPA and then stored in the dark for 30 min, the viability *E. coli* and *S. aureus* decreased to 70% and 72% respectively, demonstrating the dark toxicity of DCDPP-2TPA toward *E. coli* and *S. aureus*. Light irradiation can significantly increase the killing efficiency on both Gram-positive and -negative bacteria. The viability of *E. coli* and *S. aureus* treated with DCDPP-2TPA with room light illumination for 30 min is 10% and 14% (Fig. 5). DCDPP-2TPA based MNPs exhibited superior bacterial killing capacity, the viability was decreased to 7.5% and 9.0% respectively. All these results prove that together with light irradiation, DCDPP-2TPA based MNPs could kill both Gram-positive and -negative bacteria efficiently.

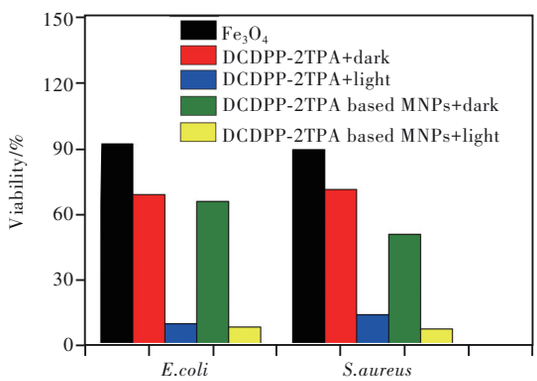

Fig. 5　Viability of *E. coli* and *S. aureus* cultured in different conditions

The stability of the DCDPP-2TPA based MNPs was tested by dynamic light scattering spectrometry. The hydrodynamic particle size showed that these nanoparticles were prone to aggregate into large particles with a particle size greater than 1 μm (Fig. S10).

The reuse of DCDPP-2TPA based MNPs bacteria killing was studied by magnetic recycling. As seen in Fig. S11, the DCDPP-2TPA based MNPs can be separated from the solution facially by magnet. After five cycles, the killing effect of *E. coli* and *S. aureus* was still obvious (Fig. S12). Note that five times is not the limit of repeatable cycles, DCDPP-2TPA based MNPs can be repeated sterilization without degrading performance.

4　Conclusion

In this paper, a magnetic antibacterial nanocomposite was facilely synthesized by incorporation of DCDPP-2TPA. The reactive oxygen species (ROS) generation property was found enhanced by AIE characteristics as well as magnetic separation

convenience. The killing bacteria capacity was proved when it was applied for Gram-negative bacteria *E. coli* and Gram-positive bacteria *S. aureus*. In particular, since the nanoparticles can be facilely separated from the solvent mixture by magnetic field, it has high potential to be used in environmental industry fields such as water disinfection system.

Supplementary Information and Response Letter are available for this paper at: http://cjl.lightpublishing.cn/thesisDetails#10.37188/CJL.20220015.

References:

[1] RAY P C, KHAN S A, SINGH A K, *et al*. Nanomaterials for targeted detection and photothermal killing of bacteria [J]. *Chem. Soc. Rev.*, 2012, 41(8): 3193-3209.

[2] MAZARI S A, ALI E, ABRO R, *et al*. Nanomaterials: applications, waste-handling, environmental toxicities, and future challenges-a review [J]. *J. Environ. Chem. Eng.*, 2021, 9(2): 105028.

[3] XING C F, XU Q L, TANG H W, *et al*. Conjugated polymer/porphyrin complexes for efficient energy transfer and improving light-activated antibacterial activity [J]. *J. Am. Chem. Soc.*, 2009, 131(36): 13117-13124.

[4] STRASSERT C A, OTTER M, ALBUQUERQUE R Q, *et al*. Photoactive hybrid nanomaterial for targeting, labeling, and killing antibiotic-resistant bacteria [J]. *Angew. Chem. Int. Ed.*, 2009, 48(42): 7928-7931.

[5] PARK S Y, BAIK H J, OH Y T, *et al*. A smart polysaccharide/drug conjugate for photodynamic therapy [J]. *Chem. Angew. Int. Ed.*, 2011, 50(7): 1644-1647.

[6] OHULCHANSKYY T Y, DONNELLY D J, DETTY M R, *et al*. Heteroatom substitution induced changes in excited-state photophysics and singlet oxygen generation in chalcogenoxanthylium dyes: effect of sulfur and selenium substitutions [J]. *J. Phys. Chem*. B, 2004, 108(25): 8668-8672.

[7] WU W B, MAO D, HU F, *et al*. A highly efficient and photostable photosensitizer with near-infrared aggregation-induced emission for image-guided photodynamic anticancer therapy [J]. *Adv. Mater.*, 2017, 29(33): 1700548-1-7.

[8] YUAN Z, LIN C C, HE Y, *et al*. Near-infrared light-triggered nitric-oxide-enhanced photodynamic therapy and low-temperature photothermal therapy for biofilm elimination [J]. *ACS Nano*, 2020, 14(3): 3546-3562.

[9] ALMEIDA A, FAUSTINO M A F, TOMÉ J P C. Photodynamic inactivation of bacteria: finding the effective targets [J]. *Future Med. Chem.*, 2015, 7(10): 1221-1224.

[10] LUO J D, XIE Z L, LAM J W Y, *et al*. Aggregation-induced emission of 1-methyl-1, 2, 3, 4, 5-pentaphenylsilole [J]. *Chem. Commun.*, 2001(18): 1740-1741.

[11] MEI J, LEUNG N L C, KWOK R T K, *et al*. Aggregation-induced emission: together we shine, united we soar [J]. *Chem. Rev.*, 2015, 115(21): 11718-11940.

[12] 张志军, 康苗苗, 王媛玮, 等. 聚集诱导发光材料在光学诊疗中的研究进展 [J]. 发光学报, 2021, 42(3): 361-378.
ZHANG Z J, KANG M M, WANG Y W, *et al*. Recent advances of aggregation-induced emission materials in phototheranostics [J]. *Chin. J. Lumin.*, 2021, 42(3): 361-378. (in Chinese)

[13] 徐晗, 王宇昕, 景靳彭, 等. 聚集诱导发光增强型金属纳米团簇在生物医学领域的研究进展 [J]. 发光学报, 2021, 42(3): 336-347.
XU H, WANG Y X, JING J P, *et al*. Progress on metal nanoclusters with aggregation-induced emission characteristic in biomedical application [J]. *Chin. J. Lumin.*, 2021, 42(3): 336-347. (in Chinese)

[14] 彭嘉琪, 陈明, 秦安军, 等. 聚集诱导发光探针用于线粒体靶向和癌细胞识别研究进展 [J]. 发光学报, 2021, 42(3): 348-360.
PENG J Q, CHEN M, QIN A J, *et al*. Progress on aggregation-induced emission probes for mitochondria target and cancer cell identification [J]. *Chin. J. Lumin.*, 2021, 42(3): 348-360. (in Chinese)

[15] WU Y H, CHEN Q X, LI Q Y, *et al*. Daylight-stimulated antibacterial activity for sustainable bacterial detection and inhibition [J]. *J. Mater. Chem*. B, 2016, 4(38): 6350-6357.

[16] CHEN S, CHEN Q X, LI Q Y, *et al*. Biodegradable synthetic antimicrobial with aggregation-induced emissive luminogens

for temporal antibacterial activity and facile bacteria detection [J]. *Chem. Mater.*, 2018, 30(5): 1782-1790.

[17] WANG Y L, CHEN M, ALIFU N, *et al.* Aggregation-induced emission luminogen with deep-red emission for through-skull three-photon fluorescence imaging of mouse [J]. *ACS Nano*, 2017, 11(10): 10452-10461.

谢宏琴(1971–),女,江苏如皋人,博士,高级工程师,2005 年于中国科学院广州地球化学研究所获得博士学位,主要从事环境监测与环境科学的研究。

E-mail: 352775029@qq.com

焦哲(1982–),女,河南漯河人,博士,副教授,2010 年于中山大学获得博士学位,主要从事基于 AIEgens 的光化学传感器的研究。

E-mail: jiaoz@dgut.edu.cn

黄雪琳(1972–),女,江西高安人,硕士,高级工程师,2001 年于南昌大学获得硕士学位,主要从事食品、环境等污染物分析方法的研究。

E-mail: 34056583@qq.com